

RESEARCH ARTICLE

## Generating multi-wavelength phase screens for atmospheric wave optics simulations using fast Fourier transforms

M. W. Hyde IV<sup>a</sup>, M. F. Spencer<sup>b,c</sup>, and M. Kalensky<sup>d</sup>

<sup>a</sup>Epsilon C5I, Beavercreek, OH, 45431, USA

<sup>b</sup>Department of Engineering Physics, Air Force Institute of Technology, Dayton, OH, 45433, USA

<sup>c</sup>Joint Directed Energy Transition Office, Office of the Under Secretary of Defense for Research and Engineering, Washington, DC, USA

<sup>d</sup>Integrated Engagement Systems Department, Naval Surface Warfare Center Dahlgren Division, Dahlgren, Virginia, USA

### ARTICLE HISTORY

Compiled May 2, 2025

### ABSTRACT

We present a method to synthesize phase screens for multi-wavelength, atmospheric wave optics simulations using fast Fourier transforms. We validate our work by comparing the theoretical, two-wavelength optical path length structure function to simulated results, and we find the two to be in excellent agreement. Our phase screen synthesis method will be useful in two-wavelength adaptive optics simulations in strong or deep turbulence.

### KEYWORDS

Adaptive optics; atmospheric turbulence; wave optics simulations

## 1. Introduction

Techniques to quickly and accurately synthesize atmospheric phase screens for use in wave optics simulations has been an active area of research for over 30 years [1–9]. For much of this history, the primary goal has been to generate an accurate, discrete representation of a continuous turbulent path at a single wavelength.

Recently, there has been interest in two- or multi-wavelength adaptive optics (AO) systems for beam projection applications [10,11]. In two-wavelength AO, the atmosphere is sensed at one wavelength and corrected at another. In astronomy, this is common practice and has been studied for decades [12–21]. However, in contrast to astronomical viewing, two-wavelength AO systems for beam projection generally operate in complementary conditions (i.e., small fields of view and long, nearly horizontal paths [22]). The latter causes scintillation which gives rise to phase discontinuities known as branch points [23,24]. The effect of these phenomena on two-wavelength AO performance has yet to be fully quantified [10].

This, of course, motivates research into two-wavelength AO systems in strong turbulence conditions and, as a consequence, techniques to generate turbulence realizations

with the proper statistics at two or more wavelengths. Indeed, the two-wavelength phase covariance function  $B_S$ , first derived by Ishimaru [25], is

$$\begin{aligned}
B_S(\boldsymbol{\rho}, k_1, k_2) &= \langle \phi(\boldsymbol{\rho}_1, k_1) \phi(\boldsymbol{\rho}_2, k_2) \rangle = \iint_{-\infty}^{\infty} \Phi_S(\boldsymbol{\kappa}, k_1, k_2) \exp(\mathbf{j}\boldsymbol{\kappa} \cdot \boldsymbol{\rho}) \, d^2\boldsymbol{\kappa} \\
\Phi_S(\boldsymbol{\kappa}, k_1, k_2) &= \pi k_1 k_2 z \Phi_n(\boldsymbol{\kappa}) \left\{ \operatorname{sinc} \left[ \frac{z}{2} \left( \frac{1}{k_1} - \frac{1}{k_2} \right) \boldsymbol{\kappa}^2 \right] + \operatorname{sinc} \left[ \frac{z}{2} \left( \frac{1}{k_1} + \frac{1}{k_2} \right) \boldsymbol{\kappa}^2 \right] \right\},
\end{aligned} \tag{1}$$

where  $\boldsymbol{\rho} = \boldsymbol{\rho}_1 - \boldsymbol{\rho}_2$ ,  $\Phi_n$  is the index of refraction power spectrum,  $z$  is the propagation distance, and  $\operatorname{sinc}(x) = \sin(x)/x$ . Letting  $k_1 = k_2 = k$  and making the approximation that the second  $\operatorname{sinc}(x)$  function is equal to one (better known as the geometrical optics approximation) simplifies Eq. (1) to the expression used for decades to generate atmospheric phase screens. However, multi-wavelength simulations involving turbulence should use the full expression in Eq. (1) to synthesize screens, as it is necessary to capture the physical correlation of the turbulent phase across the wavelengths of interest.

Charnotskii, in Ref. [26], was the first to present such a technique. Therein, he describes how to synthesize two-wavelength phase screens using the sparse spectrum (SS) method [7,8]. Our purpose in this short paper is to show how to generate such screens using the more popular Fourier or spectral method [2,5,9].

It is important to state that although the Fourier technique may be more popular than SS, Charnotskii makes compelling arguments for the superiority of the SS method in Refs. [9,26]. We do not dispute his conclusions in those papers. Rather, our purpose here is merely to generalize the existing single-wavelength Fourier method to any number of wavelengths. In what follows, we present the theory, procedure, and validation of our multi-wavelength Fourier/spectral phase screen method.

## 2. Theory

We begin with the traditional Fourier method for generating an atmospheric phase screen at a single wavenumber  $k_1 = 2\pi/\lambda_1$  [2,5,9]:

$$\begin{aligned}
\phi[i, j, k_1] &= \operatorname{Re} \left\{ \sum_{m,n} (r^r[m, n, k_1] + \mathbf{j}r^i[m, n, k_1]) \sqrt{\Phi_S[m, n, k_1, k_1]} \frac{2\pi}{L_x} \frac{2\pi}{L_y} \right. \\
&\quad \left. \times \exp\left(\mathbf{j}2\pi \frac{m}{M} i\right) \exp\left(\mathbf{j}2\pi \frac{n}{N} j\right) \right\},
\end{aligned} \tag{2}$$

where  $\operatorname{Re}(c)$  is the real part of  $c$ ;  $M, N$  are the numbers of points along the horizontal and vertical grid directions;  $i, j$  are indices corresponding to  $x, y$ ; and  $m, n$  are indices corresponding to spatial frequencies  $\kappa_x, \kappa_y$ . Also in Eq. (2),  $L_x = M\Delta x$ ,  $L_y = N\Delta y$ ,  $\Delta x, \Delta y$  are the horizontal and vertical grid spacings,  $r^r, r^i$  are  $N \times M$  matrices of independent, standard normal random numbers, and lastly,  $\Phi_S$  is the phase power spectrum in Eq. (1) [27,28]. Equation (2) is equivalent to a discrete inverse Fourier transform; therefore, the fast Fourier transform (FFT) algorithm can be used to synthesize the screen. Note that the imaginary part of the sum in Eq. (2) is statistically independent of the real part and also has the proper spatial statistics. Either or both can be used to form  $\phi$ .

Our goal is to generate other phase screens at  $k_2, k_3, \dots, k_Q$  using Eq. (2) that have the proper covariance. Proceeding, we compute the moment  $\langle \phi [i_1, j_1, k_p] \phi [i_2, j_2, k_q] \rangle$  using Eq. (2) and, after expansion, obtain

$$\begin{aligned} \langle \phi [i_1, j_1, k_p] \phi [i_2, j_2, k_q] \rangle &= \sum_{m_1, n_1} \sum_{m_2, n_2} \frac{2\pi}{L_x} \frac{2\pi}{L_y} \sqrt{\Phi_S [m_1, n_1, k_p, k_p]} \sqrt{\Phi_S [m_2, n_2, k_q, k_q]} \\ &\times \left\{ \langle r^r [m_1, n_1, k_p] r^r [m_2, n_2, k_q] \rangle \cos \left[ 2\pi \left( \frac{m_1}{M} i_1 + \frac{n_1}{N} j_1 \right) \right] \cos \left[ 2\pi \left( \frac{m_2}{M} i_2 + \frac{n_2}{N} j_2 \right) \right] \right. \\ &+ \langle r^i [m_1, n_1, k_p] r^i [m_2, n_2, k_q] \rangle \sin \left[ 2\pi \left( \frac{m_1}{M} i_1 + \frac{n_1}{N} j_1 \right) \right] \sin \left[ 2\pi \left( \frac{m_2}{M} i_2 + \frac{n_2}{N} j_2 \right) \right] \\ &- \langle r^r [m_1, n_1, k_p] r^i [m_2, n_2, k_q] \rangle \cos \left[ 2\pi \left( \frac{m_1}{M} i_1 + \frac{n_1}{N} j_1 \right) \right] \sin \left[ 2\pi \left( \frac{m_2}{M} i_2 + \frac{n_2}{N} j_2 \right) \right] \\ &\left. - \langle r^i [m_1, n_1, k_p] r^r [m_2, n_2, k_q] \rangle \sin \left[ 2\pi \left( \frac{m_1}{M} i_1 + \frac{n_1}{N} j_1 \right) \right] \cos \left[ 2\pi \left( \frac{m_2}{M} i_2 + \frac{n_2}{N} j_2 \right) \right] \right\}. \end{aligned} \quad (3)$$

Letting  $\langle r_1^r r_2^r \rangle = \langle r_1^i r_2^i \rangle$  and  $\langle r_1^r r_2^i \rangle = \langle r_1^i r_2^r \rangle$  simplifies Eq. (3) to

$$\begin{aligned} \langle \phi [i_1, j_1, k_p] \phi [i_2, j_2, k_q] \rangle &= \sum_{m_1, n_1} \sum_{m_2, n_2} \frac{2\pi}{L_x} \frac{2\pi}{L_y} \sqrt{\Phi_S [m_1, n_1, k_p, k_p]} \sqrt{\Phi_S [m_2, n_2, k_q, k_q]} \\ &\times \left\{ \langle r^r [m_1, n_1, k_p] r^r [m_2, n_2, k_q] \rangle \cos \left[ 2\pi \left( \frac{m_1}{M} i_1 + \frac{n_1}{N} j_1 - \frac{m_2}{M} i_2 - \frac{n_2}{N} j_2 \right) \right] \right. \\ &\left. - \langle r^r [m_1, n_1, k_p] r^i [m_2, n_2, k_q] \rangle \sin \left[ 2\pi \left( \frac{m_1}{M} i_1 + \frac{n_1}{N} j_1 + \frac{m_2}{M} i_2 + \frac{n_2}{N} j_2 \right) \right] \right\}. \end{aligned} \quad (4)$$

Equation (4) must equal  $B_S$  in Eq. (1) for the screens to be physical. This requires  $\langle r_1^r r_2^i \rangle = 0$  and

$$\langle r^r [m_1, n_1, k_p] r^r [m_2, n_2, k_q] \rangle = \frac{\Phi_S [m_1, n_1, k_p, k_p] \delta [m_1 - m_2] \delta [n_1 - n_2]}{\sqrt{\Phi_S [m_1, n_1, k_p, k_p]} \sqrt{\Phi_S [m_2, n_2, k_q, k_q]}}, \quad (5)$$

where  $\delta [x]$  is the Kronecker delta function. Substituting Eq. (5) into Eq. (4) and evaluating the trivial sums over  $m_2, n_2$ , we obtain the Riemann sum form of Eq. (1).

The above analysis reveals that we can synthesize phase screens at  $k_p$  and  $k_q$  with the proper, physical covariance by using correlated Gaussian random numbers in Eq. (2). Such numbers are easy to generate using Cholesky factors. Referring to Eq. (5), the covariance matrix for  $r_p^r, r_q^r$  and  $r_p^i, r_q^i$  (the real and imaginary parts are statistically independent) is equal to

$$\Sigma_{pq} = \begin{bmatrix} 1 & R_{pq} \\ R_{pq} & 1 \end{bmatrix}, \quad (6)$$

where  $R_{pq}$  is

$$R_{pq} = \frac{\Phi_S [m, n, k_p, k_q]}{\sqrt{\Phi_S [m, n, k_p, k_p]} \sqrt{\Phi_S [m, n, k_q, k_q]}}. \quad (7)$$

It is easy to generalize Eq. (6) to any number of wavenumbers, such that

$$\mathbf{\Sigma} = \begin{bmatrix} 1 & R_{12} & R_{13} & \dots & R_{1Q} \\ R_{12} & 1 & R_{23} & \dots & R_{2Q} \\ R_{13} & R_{23} & 1 & \dots & R_{3Q} \\ \vdots & \vdots & \vdots & \ddots & \vdots \\ R_{1Q} & R_{2Q} & R_{3Q} & \dots & 1 \end{bmatrix}. \quad (8)$$

The Cholesky decomposition of Eq. (8)—i.e.,  $\mathbf{\Sigma} = \mathbf{L}\mathbf{L}^T$ , where  $\mathbf{L}$  is a lower triangular matrix—is [29,30]

$$L_{qq} = \left( \Sigma_{qq} - \sum_{k=1}^{q-1} L_{qk}^2 \right)^{1/2} \quad (9)$$

$$L_{pq} = \frac{1}{L_{qq}} \left( \Sigma_{pq} - \sum_{k=1}^{q-1} L_{pk}L_{qk} \right) \quad p > q.$$

The Gaussian random numbers  $r_{1,\dots,Q}^r$  and  $r_{1,\dots,Q}^i$ , which are substituted into Eq. (2) to synthesize phase screens at  $k_1, k_2, \dots, k_Q$ , are generated from  $2Q$   $N \times M$  matrices of independent, standard normal random numbers according to

$$\begin{bmatrix} r_1^r, r_1^i \\ r_2^r, r_2^i \\ r_3^r, r_3^i \\ \vdots \\ r_Q^r, r_Q^i \end{bmatrix} = \begin{bmatrix} L_{11} & 0 & 0 & \dots & 0 \\ L_{21} & L_{22} & 0 & \dots & 0 \\ L_{31} & L_{32} & L_{33} & \dots & 0 \\ \vdots & \vdots & \vdots & \ddots & \vdots \\ L_{Q1} & L_{Q2} & L_{Q3} & \dots & L_{QQ} \end{bmatrix} \begin{bmatrix} r_1, r_{Q+1} \\ r_2, r_{Q+2} \\ r_3, r_{Q+3} \\ \vdots \\ r_Q, r_{2Q} \end{bmatrix} \quad (10)$$

with  $L_{pq}$  computed recursively using Eq. (9).

### 3. Procedure

In summary, the procedure for generating multi-wavelength phase screens using FFTs is as follows:

- (1) Generate two sets of  $Q$  standard normal random numbers.
- (2) Compute the Cholesky matrix  $\mathbf{L}$  using Eq. (9).
- (3) Generate  $r_{1,\dots,Q}^r$  and  $r_{1,\dots,Q}^i$  using Eq. (10).
- (4) Substitute  $r_{1,\dots,Q}^r$  and  $r_{1,\dots,Q}^i$  into Eq. (2).
- (5) Compute  $Q$  two-dimensional FFTs.

We note that our method can also be used to synthesize multi-wavelength subharmonic screens [2,5,9]:

- (1) Generate two sets of  $Q$  standard normal random numbers.
- (2) Compute the Cholesky matrix  $\mathbf{L}$  using Eq. (9).
- (3) Generate  $r_{1,\dots,Q}^r$  and  $r_{1,\dots,Q}^i$  using Eq. (10).
- (4) Substitute  $r_{1,\dots,Q}^r$  and  $r_{1,\dots,Q}^i$  into Eq. (10) in Ref. [9].
- (5) Compute the discrete Fourier transform.

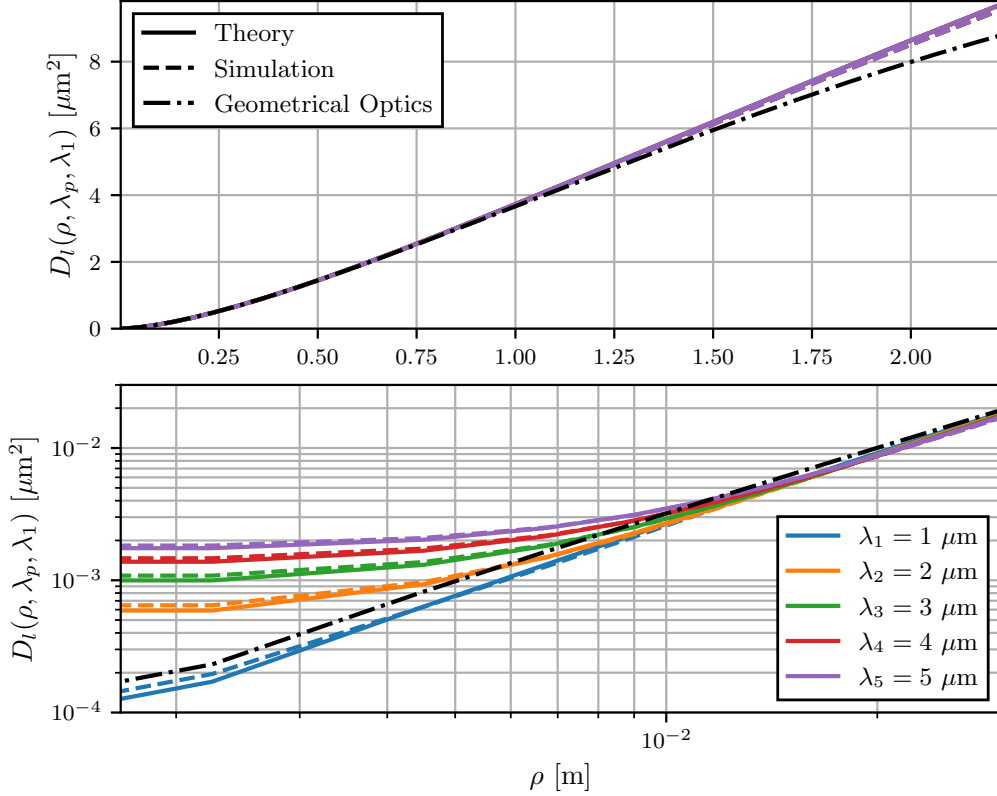


**Figure 1.** Two-wavelength OPL structure function  $D_l(\rho, \lambda_p, \lambda_1)$  results plotted on linear and log-log scales.

(6) Sum the subharmonic screens.

#### 4. Validation

Figure 1 shows the optical path length (OPL) structure function  $D_l$  results comparing simulation and theory. The theoretical  $D_l$  is given as Eq. (18) in Ref. [26], which we computed numerically with  $\Phi_n$  equal to the modified von Kármán spectrum [31],  $C_n^2 = 3.71 \times 10^{-15} \text{ m}^{-2/3}$ ,  $z = 750 \text{ m}$ ,  $l_0 = 5 \text{ mm}$ , and  $L_0 = 20 \text{ m}$ . We also included the geometrical optics (GO)  $D_l$ , which we obtained from the phase structure function  $D_S = k_p k_q D_l$  given in Chap. 6, Eq. (60) of Ref. [32]. We computed the simulated  $D_l$  from 1,000 statistically independent  $\phi$ , where the side length and pitch of the square grids were 9 m and  $l_0/3$ , respectively. Each of the 1,000  $\phi$  consisted of an FFT screen plus three subharmonic screens. We have included a Python script for generating multi-wavelength phase screens in Ref. [33].

We observe excellent agreement of the theoretical and simulated  $D_l$  in Fig. 1. The quality of these results validate our multi-wavelength Fourier phase screen method. Note that the two-wavelength structure functions do not equal zero at  $\rho = 0$  like the single-wavelength  $D_l$ . This feature is described in Ref. [26]. In addition, the single-wavelength  $D_l$  (blue trace) is below the GO  $D_l$  at small separations (bottom plot) due to diffraction, which is included in the phase power spectrum in Eq. (2).

## 5. Conclusion

In this paper, we presented a method to generate atmospheric phase screens at multiple wavelengths using FFTs. This work extended the well-established Fourier/spectral method for generating phase screens at a single wavelength and augmented the recent SS method for two-wavelength phase screens [26]. We began this short paper with a section summarizing the theory underpinning our method and concluded with a step-by-step recipe detailing how to implement our technique. We then validated our method by comparing the two-wavelength OPL structure function obtained from 1,000 screens at five wavelengths to theory. The results were in excellent accord. Our method for generating multi-wavelength phase screens will be useful in simulations studying the effects of strong turbulence on two-wavelength AO systems.

## Acknowledgment(s)

The authors would like to thank the Joint Directed Energy Transition Office for sponsoring this research.

M.W.H.: The views expressed in this paper are those of the author and do not reflect the policy or position of Epsilon C5I or Epsilon Systems.

## Disclosure statement

The author declares that the research was conducted in the absence of any commercial or financial relationships that could be construed as a potential conflict of interest.

The U.S. Government is authorized to reproduce and distribute reprints for governmental purposes notwithstanding any copyright notation thereon. Distribution Statement A. Approved for public release: distribution is unlimited. Public Affairs release approval #: NSWCDD-PN-25-00102.

## Funding

This research received no funding.

## References

- [1] Roddier NA. Atmospheric wavefront simulation using Zernike polynomials. *Opt Eng.* 1990;29(10):1174–1180. Available from: <https://doi.org/10.1117/12.55712>.
- [2] Lane RG, Glindemann A, Dainty JC. Simulation of a Kolmogorov phase screen. *Waves in Random Media.* 1992;2(3):209–224. Available from: <https://doi.org/10.1088/0959-7174/2/3/003>.
- [3] Roggemann MC, Welsh BM. *Imaging through turbulence.* Boca Raton, Florida: CRC Press; 1996.
- [4] Frehlich R. Simulation of laser propagation in a turbulent atmosphere. *Appl Opt.* 2000 Jan;39(3):393–397. Available from: <http://ao.osa.org/abstract.cfm?URI=ao-39-3-393>.
- [5] Schmidt JD. *Numerical simulation of optical wave propagation with examples in matlab.* Bellingham, Washington: SPIE Press; 2010.

- [6] Carbillet M, Riccardi A. Numerical modeling of atmospherically perturbed phase screens: New solutions for classical fast Fourier transform and Zernike methods. *Appl Opt.* 2010 Nov;49(31):G47–G52. Available from: <https://opg.optica.org/ao/abstract.cfm?URI=ao-49-31-G47>.
- [7] Charnotskii M. Sparse spectrum model for a turbulent phase. *J Opt Soc Am A.* 2013 Mar;30(3):479–488. Available from: <http://josaa.osa.org/abstract.cfm?URI=josaa-30-3-479>.
- [8] Charnotskii M. Statistics of the sparse spectrum turbulent phase. *J Opt Soc Am A.* 2013 Dec;30(12):2455–2465. Available from: <http://josaa.osa.org/abstract.cfm?URI=josaa-30-12-2455>.
- [9] Charnotskii M. Comparison of four techniques for turbulent phase screens simulation. *J Opt Soc Am A.* 2020 May;37(5):738–747. Available from: <http://josaa.osa.org/abstract.cfm?URI=josaa-37-5-738>.
- [10] Hyde MW, McCrae JE, Kalensky M, et al. “Hidden phase” in two-wavelength adaptive optics. *Appl Opt.* 2024 Jun;63(16):E1–E9. Available from: <https://opg.optica.org/ao/abstract.cfm?URI=ao-63-16-E1>.
- [11] Hyde MW, Kalensky M, Spencer MF. Phase error scaling law in two-wavelength adaptive optics. *IEEE Photonics Technol Lett.* 2024 June;36(12):779–782.
- [12] Fugate RQ, Fried DL, Ameer GA, et al. Measurement of atmospheric wavefront distortion using scattered light from a laser guide-star. *Nature.* 1991;353(6340):144–146.
- [13] Fugate RQ, Ellerbroek BL, Higgins CH, et al. Two generations of laser-guide-star adaptive-optics experiments at the Starfire Optical Range. *J Opt Soc Am A.* 1994 Jan;11(1):310–324. Available from: <https://opg.optica.org/josaa/abstract.cfm?URI=josaa-11-1-310>.
- [14] Ageorges N, Dainty C, editors. *Laser guide star adaptive optics for astronomy.* Dordrecht, Netherlands: Kluwer Academic; 2000.
- [15] Parenti RR, Sasiela RJ. Laser-guide-star systems for astronomical applications. *J Opt Soc Am A.* 1994 Jan;11(1):288–309. Available from: <https://opg.optica.org/josaa/abstract.cfm?URI=josaa-11-1-288>.
- [16] Wang L, Andersen D, Ellerbroek B. Sky coverage modeling for the whole sky for laser guide star multiconjugate adaptive optics. *Appl Opt.* 2012 Jun;51(16):3692–3700. Available from: <https://opg.optica.org/ao/abstract.cfm?URI=ao-51-16-3692>.
- [17] Lukin VP. Efficiency of some correction systems. *Opt Lett.* 1979 Jan;4(1):15–17. Available from: <https://opg.optica.org/ol/abstract.cfm?URI=ol-4-1-15>.
- [18] Hogge CB, Butts RR. Effects of using different wavelengths in wave-front sensing and correction. *J Opt Soc Am.* 1982 May;72(5):606–609. Available from: <https://opg.optica.org/abstract.cfm?URI=josa-72-5-606>.
- [19] Holmes JF, Gudimetla VSR. Strehl’s ratio for a two-wavelength continuously deformable optical adaptive transmitter. *J Opt Soc Am.* 1983 Sep;73(9):1119–1122. Available from: <https://opg.optica.org/abstract.cfm?URI=josa-73-9-1119>.
- [20] Winocur J. Dual-wavelength adaptive optical systems. *Appl Opt.* 1983 Dec;22(23):3711–3715. Available from: <https://opg.optica.org/ao/abstract.cfm?URI=ao-22-23-3711>.
- [21] Devaney N, Goncharov AV, Dainty JC. Chromatic effects of the atmosphere on astronomical adaptive optics. *Appl Opt.* 2008 Mar;47(8):1072–1081. Available from: <https://opg.optica.org/ao/abstract.cfm?URI=ao-47-8-1072>.
- [22] Kalensky M, Getts D, Banet MT, et al. Limitations of beam-control compensation. *Opt Express.* 2024 Nov;32(24):42301–42317. Available from: <https://opg.optica.org/oe/abstract.cfm?URI=oe-32-24-42301>.
- [23] Fried DL, Vaughn JL. Branch cuts in the phase function. *Appl Opt.* 1992 May;31(15):2865–2882. Available from: <http://ao.osa.org/abstract.cfm?URI=ao-31-15-2865>.
- [24] Fried DL. Branch point problem in adaptive optics. *J Opt Soc Am A.* 1998 Oct;15(10):2759–2768. Available from:

- <http://josaa.osa.org/abstract.cfm?URI=josaa-15-10-2759>.
- [25] Ishimaru A. Temporal frequency spectra of multifrequency waves in turbulent atmosphere. *IEEE Trans Antennas Propag.* 1972 Jan;20(1):10–19.
  - [26] Charnotskii M. Phase screens for the two-wave adaptive optics simulations. *Optica Open.* 2024;Preprint.
  - [27] Tatarskii VI. Wave propagation in a turbulent medium. New York, New York: McGraw-Hill; 1961.
  - [28] Ishimaru A. Wave propagation and scattering in random media. Piscataway, New Jersey: IEEE Press; 1999.
  - [29] Strang G. Linear algebra and its applications. 3rd ed. Toronto, Canada: Thomson Learning; 1988.
  - [30] Watkins DS. Fundamentals of matrix computations. 2nd ed. New York, New York: Wiley; 2002.
  - [31] Sasiela RJ. Electromagnetic wave propagation in turbulence. 2nd ed. Bellingham, Washington: SPIE Press; 2007.
  - [32] Andrews LC, Phillips RL. Laser beam propagation through random media. 2nd ed. Bellingham, Washington: SPIE Press; 2005.
  - [33] Hyde M. `Generate_Multi_Wvl_Screens.py`: Python script to synthesize multi-wavelength atmospheric phase screens. 2025 Feb;Available from: <https://doi.org/10.6084/m9.figshare.27981053.v2>.